Neuropsychopharmacology (2015) 40, 1417–1427

www.neuropsychopharmacology.org

Measuring Cigarette Smoking-Induced Cortical Dopamine Release: A [^{11}C]FLB-457 PET Study

Victoria C Wing*[1], Doris E Payer[2,3], Sylvain Houle[2], Tony P George[1,3] and Isabelle Boileau[2,3]

[1]Schizophrenia Division, Complex Mental Illness Program, and Campbell Family Mental Health Research Institute, Centre for Addiction and Mental Health (CAMH), Toronto, ON, Canada; [2]Research Imaging Centre (RIC), Campbell Family Mental Health Research Institute, Centre for Addiction and Mental Health, Toronto, ON, Canada; [3]Division of Brain and Therapeutics, Department of Psychiatry, University of Toronto, Toronto, ON, Canada

Striatal dopamine (DA) is thought to have a fundamental role in the reinforcing effects of tobacco smoking and nicotine. Microdialysis studies indicate that nicotine also increases DA in extrastriatal brain areas, but much less is known about its role in addiction. High-affinity $D_{2/3}$ receptor radiotracers permit the measurement of cortical DA in humans using positron emission tomography (PET). [^{11}C]FLB-457 PET scans were conducted in 10 nicotine-dependent daily smokers after overnight abstinence and reinstatement of smoking. Voxel-wise [^{11}C]-FLB-457-binding potential (BP_{ND}) in the frontal lobe, insula, and limbic regions was estimated in the two conditions. Paired *t*-tests showed BP_{ND} values were reduced following smoking (an indirect index of DA release). The overall peak *t* was located in the cingulate gyrus, which was part of a larger medial cluster (BP_{ND} change $-12.1 \pm 9.4\%$) and this survived false discovery rate correction for multiple comparisons. Clusters were also identified in the left anterior cingulate cortex/medial frontal gyrus, bilateral prefrontal cortex (PFC), bilateral amygdala, and the left insula. This is the first demonstration of tobacco smoking-induced cortical DA release in humans; it may be the result of both pharmacological (nicotine) and non-pharmacological factors (tobacco cues). Abstinence increased craving but had minimal cognitive effects, thus limiting correlation analyses. However, given that the cingulate cortex, PFC, insula, and amygdala are thought to have important roles in tobacco craving, cognition, and relapse, these associations warrant investigation in a larger sample. [^{11}C]FLB-457 PET imaging may represent a useful tool to investigate individual differences in tobacco addiction severity and treatment response.

Neuropsychopharmacology (2015) **40,** 1417–1427; doi:10.1038/npp.2014.327; published online 4 February 2015

INTRODUCTION

A commonality between addictive drugs, including tobacco and its primary psychoactive ingredient nicotine, is their ability to elevate extracellular dopamine (DA) levels. Nicotinic acetylcholine receptors (nAChR) are widely expressed in the brain and are abundant in the mesolimbic, nigrostriatal, and mesocortical systems (Marshall *et al*, 1997). Nicotine increases DA in limbic and striatal systems directly by activating nAChRs situated on cell bodies (Sesack and Grace, 2009) and terminals (Schilstrom *et al*, 1998) of midbrain DAergic neurons projecting from the ventral tegmental area (VTA) and substantia nigra to the nucleus accumbens and dorsal striatum, respectively, and indirectly by modulating glutamatergic and GABAergic inputs onto DAergic neurons (Mansvelder *et al*, 2003). Nicotine can also induce DA release in the prefrontal cortex (PFC) via stimulation of nAChRs located on the cell bodies on DAergic neurons projecting from the VTA to the PFC (George *et al*, 2000) and via nAChRs in the PFC (Livingstone *et al*, 2009). However, studies using *in vivo* microdialysis to directly compare the regional effects of nicotine on DA dialysate report greater release in the striatum and nucleus accumbens compared with the PFC. For example, relative to the PFC, nicotine-induced DA release is 2 and 10 times greater in the striatum and nucleus accumbens of rodents and 1.3 times greater in the striatum of non-human primates (Domino and Tsukada, 2009; Marshall *et al*, 1997).

The ability of nicotine to increase DA release in the (limbic) striatum is thought to underlie its reinforcing and euphoric effects (Di Chiara, 2000), a view that finds partial support from neuroimaging studies showing that tobacco-induced DA release is associated with decreased craving (Brody *et al*, 2004; Le Foll *et al*, 2014), and withdrawal symptoms (Le Foll *et al*, 2014), elevated mood (Barrett *et al*, 2004), and motivation to smoke (ie, puff volume) (Le Foll *et al*, 2014). The role of cortical DA in tobacco addiction is less well understood but may relate to nicotine's pro-cognitive effects. In this regard, it has been proposed that

*Correspondence: Dr VC Wing, Schizophrenia Division, Complex Mental Illness Program, and Campbell Family Mental Health Research Institute, Centre for Addiction and Mental Health (CAMH), Toronto, ON, Canada M5T 1R8, Tel: +1 44 746 264 7320,
E-mal: Victoria.Wing13@imperial.ac.uk
Received 17 May 2014; revised 4 December 2014; accepted 4 December 2014; accepted article preview online 15 December 2014

cognitive dysfunction associated with nicotine withdrawal (Levin *et al*, 2006), although variable and not reported in all populations (Sacco *et al*, 2005; Wing *et al*, 2013b), contributes to the addictive nature of tobacco smoking (Ashare *et al*, 2014; Heishman *et al*, 2010) and may be related cortical DA dysfunction. Brain-imaging studies (functional magnetic resonance imaging (fMRI), fludeoxyglucose, and oxygen-15 positron emission tomography (PET)) partly support this by showing that tobacco smoking increases brain activity in DA projection areas including the hippocampus, amygdala, insula, anterior cingulate cortex (ACC), orbitofrontal and dorsolateral PFC (dlPFC) (Azizian *et al*, 2010; Brody *et al*, 2002; Janes *et al*, 2010a; Janes *et al*, 2010b; Janes *et al*, 2013; Zubieta *et al*, 2005). These changes have been associated with improved cognitive performance (but also cue-reactivity, craving, and relapse susceptibility). Although informative, such studies do not address the question of cortical DA's involvement, if any, in tobacco addiction and there are no *in vivo* PET studies investigating whether nicotine or tobacco leads to detectable changes in DA levels in the cortex.

The development of the high-affinity D2/3 receptor radiotracers [^{18}F]-Fallypride (Mukherjee *et al*, 1995) and [^{11}C]-FLB-457 (Halldin *et al*, 1995) has allowed investigation of DA dynamics in cortical areas of living humans. This method is based on the principle that challenges that increase synaptic DA decrease radiotracer binding (compared with baseline). [^{11}C]-FLB-457 appears to show greater sensitivity to DA changes in low-receptor-density cortical regions than [^{18}F]-Fallypride (Narendran *et al*, 2009) and shows good test–retest reproducibility (Narendran *et al*, 2013). [^{11}C]-FLB-457 has been used in humans to index DA release induced by oral amphetamine, with effects measurable in four out of the eight cortical regions examined: the ACC, medial temporal lobe, dlPFC, medial PFC (mPFC) and parietal cortex (PC) (Narendran *et al*, 2009). Moreover, combined PET-microdialysis studies in non-human primates have confirmed that the amphetamine-induced reductions in [^{11}C]-FLB-457 binding correlate with direct measurement of DA release (Narendran *et al*, 2014).

In this study we used [^{11}C]-FLB-457 to index extrastriatal DA release induced by tobacco smoking. As this was the first study to attempt to measure cortical DA release induced by tobacco or nicotine, we implemented a design that we thought would evoke the maximal DA release. Thus, we examined the effects of the act of smoking tobacco following a period of (overnight) abstinence in tobacco-dependent daily smokers, therefore encompassing pharmacological (ie, nicotine) and non-pharmacological factors (ie, tobacco cues). Analyses were restricted to the prefrontal, limbic, and insular regions, which are involved in cognitive control, interoceptive awareness, and emotion. These regions of interest (ROIs) were selected based on functional brain-imaging studies of tobacco smoking (Brody *et al*, 2002; Janes *et al*, 2010a; Janes *et al*, 2010b; Janes *et al*, 2013) and [^{11}C]-FLB-457 studies showing BP_{ND} changes are measurable in these ROIs after a DA-elevating challenge (Narendran *et al*, 2009). The exploratory aim of the study was to investigate correlations between DA release and smoking behavior (assessed by smoking topography), tobacco craving, withdrawal, and cognitive function.

MATERIALS AND METHODS

Participants

All procedures were approved by the Centre for Addiction and Mental Health Research Ethics Board, and complied with ethical standards of the 1975 Helsinki Declaration (5th revision, 2000). Subjects were recruited from the local community in Toronto, Canada, using internet advertisements, and provided written informed consent. Subjects were paid $350 for study completion, including $50 for successful overnight abstinence, a paradigm that has resulted in >90% success in achieving overnight abstinence in similar populations of smokers (Sacco *et al*, 2005; Wing *et al*, 2013b).

All subjects met the following criteria: smoking ⩾10 cigarettes per day (CPD) assessed by self-reported 7-day timeline follow-back measures (Sobell *et al*, 1988), expired breath carbon monoxide (CO) ⩾10ppm, plasma cotinine levels ⩾150 ng/ml, Fagerstrom Test of Nicotine Dependence score ⩾4 (Heatherton *et al*, 1991), ⩾80 on the Shipley-2 estimate of Full Scale IQ (Zachary *et al*, 1985), and a negative urine pregnancy test and 7-panel toxicology screen for drugs of abuse (Medtox; Wilmington, NC). Subjects were screened using the Structured Clinical Interview for DSM-IV Axis I Disorders (First *et al*, 1996) and demonstrated no Axis I diagnosis with the exception of past major depression or drug and alcohol abuse if in remission for at least 1 year. Pack-years provided measures of lifetime tobacco exposure (the number of years smoked multiplied by the average number of packs of 20 CPD) (Wood *et al*, 2005). Mood symptoms were assessed using the Beck Depression Inventory (Beck *et al*, 1996). Exclusion criteria included major medical problems and PET or MRI contraindications (eg, metal implants, pregnancy/lactation, and exposure to radiation above permissible dose).

Study Design

Eligible subjects were invited for a baseline visit including a cognitive training session to minimize practice effects in the subsequent testing sessions (Figure 1). Subjects were asked to remain abstinent from 2100 h on the day before the PET scanning, which was biochemically verified by an expired CO level <10 ppm on arrival at the laboratory at 0830 h; values above this led to scan cancellation. Subjects then remained abstinent and under supervision until 1300 h (16 h). Abstinence was later confirmed by analysis of plasma nicotine levels (see next section). Subjects were also asked not to use alcohol 24 h before the scan and not to drink caffeinated drinks on the day of the scan. A further urine sample was collected to rule out pregnancy and drug use immediately before the scan.

Subjects underwent two virtually identical sessions on the testing visit: (1) at 0830–1230 h under smoking abstinence conditions and (2) at 1330–1730 h following reinstatement of smoking. Each session started with assessments of tobacco craving and withdrawal, followed by a [^{11}C] FLB-457 PET scan (4 h between the am and pm injections) and then a neuropsychological testing battery. Subjects smoked their own brand cigarettes *ad libitum* immediately before the second PET scan; the average time between starting smoking and tracer injection was 31.8 ± 7.5 min. Subjects

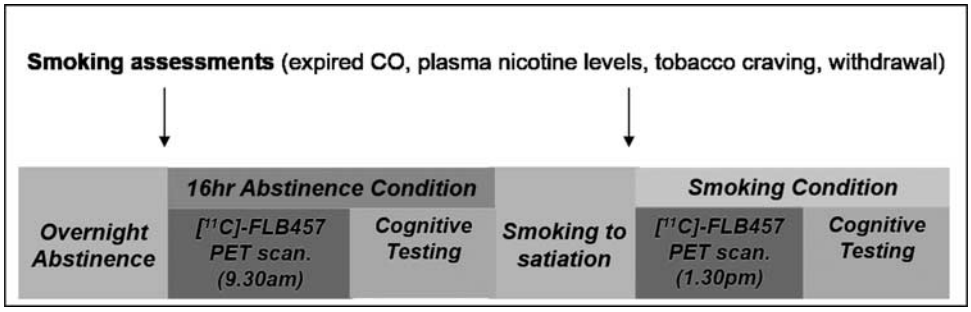

Figure 1 Single subject timeline.

were instructed to smoke as many cigarettes as they liked, to ensure they were fully satiated before PET scanning.

On a separate visit, subjects underwent a proton density weighted 3T MRI scan for spatial realignment and normalization of PET images and localization of ROIs (General Electric, 3T MR750; slice thickness, 2 mm; interleaved; number of slices, 84; repetition time, 6000 ms; echo time, 8 ms; number of excitations, 2; acquisition matrix, 256 × 192; FOV, 22 × 16.5 cm).

Plasma Nicotine and Cotinine Determination

A blood sample was obtained immediately after tracer injection in both the abstinent and smoking conditions, to determine nicotine and cotinine concentration (ng/ml). The methods used were developed in-house based on Bernert *et al* (1997). Serum samples were deproteinized and extracted at an alkaline pH with a solvent mixture using extraction devices containing diatomaceous earth. The extracts were further analyzed by liquid chromatography using mass spectroscopy detection. Deuterated analytes were used as internal standards and the calibration range is from 1 to 500 ng/ml. Between-day precision coefficients of variation at concentrations of 221 ng/ml cotinine and 23 ng/ml nicotine were $<5\%$ and 12%, respectively.

Smoking Topography

Smoking topography measures cigarette smoking behavior, specifically the intensity of smoking indexed by number of puffs, puff volume, puff duration, and interpuff interval. A Clinical Research Support System Pocket device (Borgwaldt KC, Richmond, VA) was used to assess smoking topography during the pre-scan smoking reinstatement session. Subjects were familiarized to the device during a baseline training session.

Craving and Cognitive Measures

Craving and withdrawal were assessed respectively by the self-report Tiffany Questionnaire for Smoking Urges (TQSU) (Tiffany and Drobes, 1991) and the Minnesota Nicotine Withdrawal Scale (MNWS) (Hughes and Hatsukami, 1986). The 1-h neuropsychological test battery assessed a range of cognitive domains that have been shown to be sensitive to nicotine and related to cortical DA levels: sustained attention (Conner's Continuous Performance Test), visuospatial working memory (Spatial Delayed Response Test), verbal working memory (Digit Span–Backward), Processing Speed (Trail Making Test-A) and executive function (Wisconsin Card Sorting Task; Trail Making Test-B).

PET Scan Parameters

PET scans were performed using a high-resolution PET camera system (CPS-HRRT, Siemens Medical Imaging, Knoxville, TN, USA), which measures radioactivity in 207 brain sections with a slice thickness of 1.2 mm each and an in-plane resolution of ~2.8 mm full-width at half maximum (FWHM). A custom fitted thermoplastic mask was used to reduce head movement (TruScan Imaging, Annapolis, USA). Attenuation correction was done via a transmission scan, which used a ^{137}Cs (T2 = 30.2 yr, Eγ = 622KeV) single-photon point source. Emission data were acquired in list mode for 90 min beginning after a (2 min) bolus injection (followed by a flush with 2 ml saline) of [^{11}C]FLB-457 (mean ± SD, dose: 9.57 ± 0.85 mCi; specific activity: 3227 ± 1256 mCi/μmol; mass injected: 1.25 ± 0.45 μg). Emission data were reconstructed by 2D filtered back projection to yield dynamic images with 15 1-min frames and 15 5-min frames.

PET Scan Analysis

[^{11}C] FLB-457 BP_{ND} was calculated voxel-wise across the whole brain using the basis function implementation of simplified reference tissue model (SRTM) (Gunn *et al*, 1997; Lammertsma and Hume, 1996). Despite some studies reporting detectable D2/3-receptor-specific [^{11}C]-FLB-457 binding in the cerebellum (Asselin *et al*, 2007; Delforge *et al*, 1999), the tissue time activity curve (TAC) of the cerebellar cortex (excluding vermis) was used as the reference region, because it has been deemed suitable for the calculation of [^{11}C]-FLB-457 BP_{ND} in several studies (Ito *et al*, 2001; Narendran *et al*, 2011a; Olsson *et al*, 2004; Vilkman *et al*, 2000). This approach yielded maps of [^{11}C]-FLB-457 BP_{ND} for the abstinent and smoking conditions, which were registered to each individual's MRI, transformed into standardized stereotaxic space (the ICBM 305 template), and spatially smoothed with a 6-mm FWHM kernel. These images were then entered into a group analysis and statistically investigated at every voxel using paired *t*-tests in SPM 8 (Wellcome Trust Centre for Neuroimaging, London, UK). To minimize multiple comparisons and given our *a priori* regional hypotheses, voxels investigated for

significant effects were limited to gray matter in the frontal lobe, insula, and limbic regions, using a mask generated by the WFU PickAtlas function in SPM8 (Maldjian *et al*, 2003). Within this mask, only voxels with a BP_{ND} value greater than 0.1 were considered. [^{11}C]-FLB-457 BP_{ND} maps were assessed for the contrast of interest (abstinence > smoking) at an uncorrected threshold of $p<0.05$ with a minimum 50-voxel cluster extent. This approach was chosen, as it provides a good balance between Type I and Type II error, and previous work has shown that a lenient threshold and cluster extent can produce similar results to false discovery rate (FDR) correction in fMRI studies (Lieberman and Cunningham, 2009). Individual BP_{ND} values for the abstinence and smoking conditions were then extracted from clusters surviving this threshold and used to calculate percent change in BP_{ND} between conditions. This analysis was followed up by investigating changes in [^{11}C]-FLB-457 BP_{ND} in anatomically defined whole ROIs (see Rusjan *et al* (2006) for methods).

Statistical Analysis

Statistical analyses were conducted in in SPSS (v.15.0; Chicago, IL); significance was set at $p<0.05$. Smoking and cognitive outcome measures were analyzed using paired *t*-tests to compare values in the abstinent and smoking conditions. The percentage changes in BP_{ND} extracted from the voxel-wise analyses were used in Pearson correlation analyses, to explore associations with smoking topography measures and smoking-related changes in craving, withdrawal, and cognitive function. Control analyses involved *t*-tests to evaluate possible differences in PET scan parameters between the conditions (ie, dose injected, mass injected, specific activity injected, and the cerebellar TAC) and correlation analyses to determine whether there was any relationship between mass injected and [^{11}C]-FLB-457 BP_{ND}.

RESULTS

Subject Characteristics

Eleven subjects met the eligibility criteria and were enrolled, and one subject withdrew during the first scan due to claustrophobia, resulting in a final sample of $N=10$. The demographic characteristics and PET scan parameters for the sample are presented in Table 1. There were no statistically significant differences between the PET scan parameters for the abstinent and smoking scans: amount injected 9.65 ± 0.89 mCi *vs* 9.48 ± 0.84 mCi ($p=0.66$), specific activity at time of injection 3354 ± 1451 mCi/μmol *vs* 2901 ± 994 mCi/μmol, and injected mass 1.16 ± 0.49 μg *vs* 1.33 ± 0.42 μg ($p=0.40$). Subjects smoked an average of 1.9 ± 0.6 cigarettes before the afternoon PET scan (range 1–3 cigarettes).

PET [^{11}C] FLB-457 Binding Results

We observed significant reductions in [^{11}C]-FLB-457 BP_{ND} following smoking (an indirect measure of DA release) in a set of regions that comprises a large medial cluster (cingulate gyrus, ACC, medial frontal gyrus (Med. FG), superior frontal gyrus, and precuneus), the left (L) ACC/Med. FG, the right (R) PFC/middle frontal gyrus (MFG), an L PFC cluster (precentral gyrus and MFG), the L MFG/precentral gyrus, bilateral amygdala/uncus, and the left insula (see Table 2 and Figure 2a). The overall peak *t*-value was located in the cingulate gyrus of the medial cluster and this survived FDR correction for multiple comparisons. In addition, an analysis thresholded at $p<0.01$ FDR for multiple comparisons yield only one cluster of significance, the cingulate gyrus (see * in Table 2). The reverse contrast (abstinence < smoking) did not yield any significant clusters. Individual BP_{ND} values were extracted from these clusters and are presented for illustrative purposes (see Figure 2b). These values were used to calculate percentage changes in BP_{ND} (mean ± SD) in smoking *vs* abstinence conditions: medial cluster, which included the cingulate cortex ($-12.1\pm9.4\%$), L ACC/Med. FG ($-11.0\pm11.7\%$), bilateral PFC clusters (R: $-11.5\pm12.8\%$; L: $-9.8\pm11.0\%$), bilateral amygdala/uncus (R: $-13.8\pm14.7\%$; L: $-12.0\pm13.1\%$), and the left insula ($-6.2\pm7.0\%$).

The results of the anatomically defined whole ROIs analysis is shown in Supplementary Figure 1. In brief, pairwise comparisons (one-tailed uncorrected) revealed trend-level significant decreases in [^{11}C]-FLB-457 BP_{ND} in the mPFC (-7.1%; $p=0.08$), ACC (-7.6%; $p=0.06$), and amygdala (-9.8%; $p=0.06$) but not the dlPFC or insula. Regions examined in amphetamine [^{11}C]-FLB-457 PET studies were also tested (Narendran *et al*, 2009; Narendran *et al*, 2013); similar to these studies no effect was found in the temporal or occipital cortex, but in contrast no change in BP_{ND} was found in the PC.

Smoking-Related Measures

The relationship between baseline smoking behavior and percentage change in [^{11}C] FLB-457 BP_{ND} (abstinence *vs* smoking) was investigated. A younger age of smoking onset was associated with a greater reduction in BP_{ND} in the right amygdala ($r=0.731$, $p=0.016$) and higher levels of daily smoking were associated with greater BP_{ND} reduction at the trend level in the medial cluster, which included the cingulate gyrus ($r=-0.584$, $p=0.08$) and the R PFC/MFG cluster ($r=-0.612$, $p=0.06$). Tobacco craving (TQSU Factor 1 and 2 scores) and withdrawal (MNWS total score) were significantly higher in the abstinent *vs* reinstatement session (see Table 1) but the percentage change did not correlate with the percentage change in [^{11}C] FLB-457 BP_{ND}. Time between smoking and PET scanning and changes in plasma nicotine levels after smoking reinstatement also did not correlate with changes BP_{ND}. However, the average puff volume in the smoking reinstatement session did correlate with changes in BP_{ND} (valid smoking topography data was collected in 8 out of the 10 subjects). Greater puff volumes were correlated with greater BP_{ND} reductions in the medial cluster, which included the cingulate gyrus ($r=-0.835$, $p=0.012$, see Supplementary Figure 2), L ACC/Med. FG ($r=-0.961$, $p<0.001$) and R PFC/MFG cluster ($r=-0.807$, $p=0.015$).

Cognitive Measures

Although performance in most cognitive domains was higher in the smoking *vs* abstinence conditions, this

Table 1 Subject Characteristics and PET Scan Parameters Under Abstinence and Smoking Conditions ($n = 10$)

Demographic and baseline characteristics	
Sex (Male:Female)	7:3
Race (White:Black:Hispanic:Other)	6:0:2:2
Age (years)	42.5 ± 11.1
Years of education	14.6 ± 2.5
Shipley IQ	97.1 ± 11.0
CPD	16 ± 4.7
Expired carbon monoxide (ppm)	20 ± 6.7
Pack-years (years*pack of 20/day)	19.4 ± 10.6
FTND	6.0 ± 1.1
BDI total score	2.4 ± 2.8

	Testing visit measures		
	Abstinence	**Smoking**	***P*-value**
Smoking measures			
Expired carbon monoxide (ppm)	6.8 ± 3.0	13.6 ± 4.5	**0.001**
Plasma cotinine (ng/ml)	202 ± 49	189 ± 65	0.63
Plasma nicotine (ng/ml)	1.6 ± 1.3	14.6 ± 4.9	**<0.001**
TQSU factor 1	6.1 ± 0.7	3.7 ± 0.9	**<0.001**
TQSU factor 2	5.0 ± 1.3	3.2 ± 1.1	**<0.001**
MNWS total score	10.6 ± 5.0	3.9 ± 3.2	**<0.001**
Cognitive measures			
CPT—% hits	99.2 ± 2.0	99.8 ± 0.3	0.33
CPT—% commissions	38.2 ± 23.9	30.6 ± 19.1	0.44
CPT—variability index	7.4 ± 3.9	4.2 ± 1.5	**0.03**
SDR—5 s delay	18.0 ± 6.8	25.2 ± 7.3	0.95
SDR—15 s delay	25.2 ± 7.3	19.9 ± 5.6	0.09
SDR—30 s delay	24.8 ± 8.4	19.9 ± 5.6	0.16
HVLT—total recall (test 1–3)	24.4 ± 6.4	24.9 ± 4.7	0.85
HVLT—delayed recall	8.6 ± 3.7	8.3 ± 2.9	0.84
TMT—trial A (seconds)	25.4 ± 7.3	22.2 3.6	0.24
TMT—trial B (seconds)	62.4 ± 31.9	49.7 ± 8.9	0.24
Digit span—forwards	11.9 ± 1.6	11.3 ± 2.2	0.50
Digit span—backwards	8.6 ± 2.2	8.5 ± 2.6	0.93
WCST—% total errors	25.2 ± 25.2	19.2 ± 17.0	0.54
WCST—% perseverative errors	18.0 ± 22.5	12.0 ± 12.1	0.47
PET scan parameters			
Amount injected (mCi)	9.65 ± 0.89	9.48 ± 0.84	0.66
Specific activity at T.O.I (mCi/μmol)	3554 ± 1451	2901 ± 994	0.27
Mass injected (μg)	1.16 ± 0.49	1.33 ± 0.42	0.40
AUC for cerebellum TAC	997412 ± 254915	851629 ± 165309	0.17

Abbreviations: BDI, Beck Depression Inventory; CPD, cigarettes per day; CPT, Continuous Performance Test; FTND, Fagerstrom Test for Nicotine Dependence; HVLT, Hopkins Verbal Learning Test; SDR, Spatial Delayed Response; TQSU, Tiffany Questionnaire of Smoking Urges; MNWS, Minnesota Nicotine Withdrawal Scale; VAS, Visual Analogue Scale; TAC, time activity curve; WCST, Wisconsin Card Sorting Test.
Values are stated as mean ± SD, except for sex and race; *p*-values are for paired Student's *t*-tests between the abstinence and smoking conditions (values < 0.05 are shown in bold).

difference only reached statistical significance for the CPT variability index (a measure of 'within respondent' response-speed consistency across the 18 test segments in relation to the individual's overall reaction time SE) ($t(18) = 2.39$, $p = 0.03$)). After correcting for multiple comparisons, there were no significant correlations between

Table 2 Spatial Coordinates and Statistics of the Clusters Identified in the Voxel-Wise [^{11}C]-FLB-457 BP_{ND} Abstinence > Smoking, $n = 10$

Region	Number of voxels	Brodmann	Peak coordinates (MNI space)			Peak *t*	Peak *p*
			x	*y*	*z*		
Medial cluster	1331						0.013 (cluster level)
Cingulate gyrus		24	4	10	42	5.32	<0.001[a]
		32	6	14	42	4.51	0.002
		31	−12	−30	46	3.55	0.003
Anterior cingulate		32	2	38	16	2.93	0.008
		24	6	42	−4	2.32	0.022
Medial frontal gyrus (Med. FG)		6	−6	−6	50	3.83	0.002
		9	10	52	22	3.47	0.004
		8	8	30	44	2.27	0.024
Superior frontal gyrus		6	14	38	48	3.17	0.006
		9	12	56	22	3.08	0.007
		8	8	46	42	1.99	0.038
Precuneus		7	−6	−28	50	3.90	0.002
L ACC/Med. FG	148	10/9/32	−10	48	16	3.45	0.004
R PFC/middle frontal gyrus (MFG)	323	9	38	34	26	3.38	0.004
		8	30	32	36	2.47	0.018
L PFC cluster	612						0.075 (cluster-level)
Precentral gyrus		4	−26	−16	60	3.84	0.002
MFG		8	−28	24	48	3.57	0.003
		10	−36	48	20	2.76	0.011
		6	−18	8	64	2.69	0.012
		9	−26	44	30	2.21	0.027
L MFG/precentral gyrus	88	6	−44	2	34	2.50	0.017
		4	−50	−2	44	2.24	0.026
L amygdala/uncus	76		−24	0	−30	3.28	0.005
R amygdala/uncus	98		26	−4	−30	3.03	0.007
L insula	58		−40	−12	4	2.54	0.016

Abbreviations: ACC, anterior cingulate cortex; BP_{ND}, binding potential; FDR, false discovery rate; PFC, prefrontal cortex; Med. FG, medial frontal gyrus; MFG, middle frontal gyrus; R, right; L, left.
Uncorrected *P*-values.
[a]Survived FDR correction for multiple comparisons at $p < 0.01$.

the percentage change in cognitive performance and reductions in [^{11}C] FLB-457 BP_{ND} following reinstatement of cigarette smoking.

DISCUSSION

Nicotine, the primary psychoactive ingredient in tobacco, has been shown to induce cortical DA release in animal microdialysis studies, but to our knowledge this is the first demonstration in humans of cortical DA release following tobacco smoking. [^{11}C]-FLB-457 BP_{ND} values were reduced following smoking (an indirect index of DA release). The overall peak *t* in voxel-wise analyses was located in the cingulate gyrus, which was part of a large medial cluster (percentage change in BP_{ND} $-12.1 \pm 9.4\%$) and this survived FDR correction for multiple comparisons ($p < 0.01$). There was also evidence for release in the left ACC/Med. FG, right and left PFC, bilateral amygdala/uncus, and the left insula, but these results did not survive corrections for multiple comparisons. The results of the voxel-wise analysis were also in the most part supported by an anatomically defined ROI analysis.

Microdialysis studies suggest that amphetamine elicits substantially greater DA release than nicotine and [^{11}C]raclopride, and [^{11}C]-(+)-PHNO displacement in humans tends to be greater following amphetamine *vs* nicotine, albeit to a much lesser extent (~2-fold) than observed by microdialysis (Boileau *et al*, 2014; Brody *et al*, 2009; Gallezot *et al*, 2014; Le Foll *et al*, 2014; Shotbolt *et al*, 2012). However, the smoking-induced changes in extrastriatal [^{11}C]FLB-457 binding identified in this study were of similar magnitude to those following an oral amphetamine challenge (~7–13%) (Narendran *et al*, 2009; Narendran *et al*, 2013). Combined microdialysis and *in vivo* binding studies are informative in this regard. Such studies have found that although extrasynaptic DA release induced by both methamphetamine and nicotine correlates with

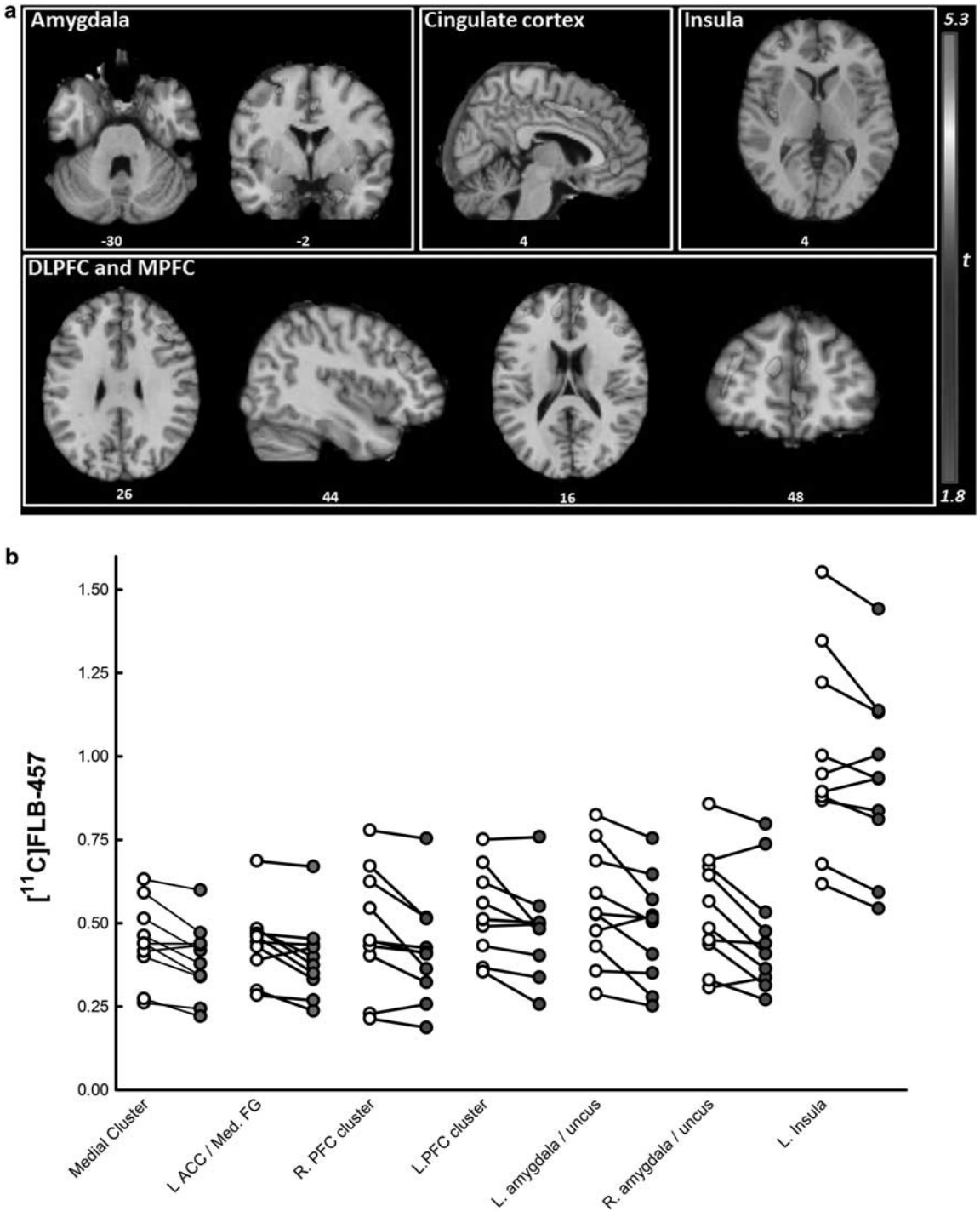

Figure 2 [11C]FLB-457-binding potential (BP_{ND}) in abstinence and smoking conditions ($n = 10$). (a) Clusters surviving a threshold of $P < 0.05$ (uncorrected)/$k > 50$ for the abstinence > smoking contrast. Clusters identified in the insula, amygdala, cingulate, and prefrontal cortex (PFC) are overlaid onto a single subject T1-weighted magnetic resonance imaging (MRI; in MNI space). Coordinates below each view are in MNI space. (b) Extracted [11C]FLB-457 BP_{ND} values for significant clusters in the voxel-wise comparison of abstinent (open circles) and smoking conditions (closed circles). ACC, anterior cingulate gyrus; L, left; Med. FG, medial frontal gyrus; MPFC, medial PFC; R, right.

reductions in [^{3}H]raclopride binding, decreases in radioligand binding per unit increase of DA were greater for nicotine than methamphetamine (Kim and Han, 2009). In rats, methamphetamine (5 mg/kg) and nicotine (3.5 mg/kg) led to substantially different changes in dialysate levels (increases of 826% after amphetamine *vs* 51% after nicotine) but elicited similar effects on [^{3}H]raclopride binding (~30% decrease) (Kim and Han, 2009). These findings may be due to the fact that changes in radioligand binding after a drug challenge presumably reflect changes within the synapse where fluctuations in DA are rapid and of significant magnitude, while microdialysis measures

extrasynaptic DA concentrations (discussed in Laruelle (2000)). Thus, the difference in the extrasynaptic DA-[^{3}H]raclopride binding relationship following nicotine and methamphetamine administration is likely the result of their different properties at DA and noradrenaline transporters (DAT and NET), which are primarily responsible for controlling extracellular DA levels in the striatum and the cortex respectively (Kim and Han, 2009).

In a recent combined microdialysis PET imaging study in non-human primates, a 1% reduction in BP_{ND} following amphetamine challenge reflected a 57% increase in cortical DA (Narendran *et al*, 2014). However, it is not possible to extrapolate this finding to our BP_{ND} changes following tobacco smoking, because, as described above, microdialysis measurements of extrasynaptic DA concentration are not a good reflection of intrasynaptic radiotracer displacement across drug classes. Another observation from the current study is that magnitude of tobacco's effects in cortical regions appear to be within the same range as those in the striatum, despite the lower DA innervation of cortical regions. Narendran *et al* (2014) demonstrated that this is likely a sensitivity issue whereby lower baseline DA levels in the cortex *versus* the striatum results in greater [^{11}C]-FLB-457 'displacability.' Different dynamics of DA release in the cortex (prolonged) and in the striatum (fast) may also explain the similar magnitude of BP_{ND} changes found between these regions (Garris and Wightman, 1994). Combined PET/microdialysis studies after smoking/nicotine challenge would help address these issues.

The regions identified in this study (ie, cingulate gyrus, ACC, Med. FG, PFC, amygdala, and insula) are consistently associated with tobacco cue-presentation and subjective craving in functional brain-imaging studies (Brody *et al*, 2002; Janes *et al*, 2010b; Janes *et al*, 2013; Zubieta *et al*, 2005), as well as some of tobacco's pro-cognitive effects (Azizian *et al*, 2010). Greater [^{11}C]-FLB-457 BP_{ND} displacement following smoking was correlated with higher puff volumes in the smoking reinstatement session, which may have resulted in higher nicotine intake and/or be a reflection of greater addiction severity. The rise in plasma nicotine levels was not correlated with BP_{ND} changes, which may be due to the time of measurement ($\sim$30 min post smoking) and the modest rise in nicotine levels observed at this time point ($\sim$13 ng/ml). There were also weak correlations with baseline smoking behavior. Tobacco-induced changes in [^{11}C]-FLB-457 BP_{ND} were not correlated with the reduction in craving following resumption of smoking. However, this may have been the result of the relatively small sample size ($n = 10$), and thus the role of cortical DA in tobacco craving remains unclear.

The role of cortical DA in cognitive function, particularly working memory and executive function, is relatively well characterized (eg, Aalto *et al* (2005), Castner and Goldman-Rakic (2004), and Ko *et al* (2009)). It is hypothesized that nicotine-induced increases in cortical DA levels contribute to its pro-cognitive effects, and conversely low cortical DA underlies the cognitive dysfunction seen in withdrawal. In this sample there were only minimal effects of tobacco abstinence on cognition which, limited correlation analyses. Nevertheless, these findings support previous studies reporting minimal effects of tobacco abstinence on cognition in healthy non-psychiatric populations (Sacco *et al*, 2005; Wing *et al*, 2013b). Certain subgroups of smokers, however, appear to show more consistent/robust withdrawal-related cognitive dysfunction such as patients with schizophrenia, a disorder associated with cortical hypodopaminergia (for review, see Wing *et al* (2012)), or those carrying the catechol-*O*-methyltransferase (COMT) Val^{158}Met polymorphism Val-allele, which is associated with low cortical DA (Loughead *et al*, 2009; Wing *et al*, 2013a). Thus, a susceptibility to tobacco's cognitive effects may be the result of a cortical hypodopaminergic state, which is corrected by tobacco; [^{11}C]-FLB-457 may be an appropriate tool to test this hypothesis.

This study has several limitations. First, due to institutional policy requiring subjects to smoke in a designated negative pressure smoking room, there was an average of 32 min between the resumption of smoking and the injection of tracer, and therefore 2 h to the end of PET scanning. Nevertheless, microdialysis studies of nicotine-induced DA release suggest 30 min post exposure is ideal to detect changes in DA, which can last up to 2 h (Domino and Tsukada, 2009) and PET imaging in non-human primates report the reduction in BP_{ND} observed following nicotine infusion dissipates after 2.5 h (Marenco *et al*, 2004). Moreover, this design was very similar to a previous study in which [^{11}C]-PHNO was used to successfully detect striatal DA release following smoking, thus suggesting this is an appropriate assessment window (Le Foll *et al*, 2014). Second, the order of the smoking conditions was non-randomized, which may have led to an effect of time of day or novelty. Although DA has been shown to have a circadian rhythms (light–dark cycles; eg, Paulson and Robinson (1994)), it is not known whether the 4 h time difference between the scans affected the finding. The effect of novelty or increased anxiety during the first scan could have increased DA levels (Nagano-Saito *et al*, 2013); however, this would have limited our chances of seeing an effect and is therefore unlikely to explain the finding. This design was therefore chosen to limit dropout and reduce variability associated with testing on separate days. A third potential limitation of this study is the use of the cerebellum as a reference region and possible carryover mass across scans due to remaining radiotracer. Although some investigators use similar methods, there is evidence for specific binding in this region (Narendran *et al*, 2011a) and others use an arterial input function to model [^{11}C]-FLB-457 BP_{ND}; this remains a subject of debate in the field. Nevertheless, [^{11}C]-FLB-457 has been shown to have acceptable test–retest variability ($\leqslant$15%) and low carryover mass effects if scans are done more than 195 min apart (Narendran *et al*, 2014; Narendran *et al*, 2011b; Sudo *et al*, 2001). Although the average [^{11}C]-FLB-457 mass injected in our study was slightly higher than that in the aforementioned studies, it did not differ between the two conditions and did not correlate with the [^{11}C]-FLB-457 BP_{ND} results.

We chose to use a voxel-wise *vs* a ROI approach, as it is without anatomical constraints and therefore facilitates the capture of terminal DA fields in cortical areas that are known to have a complex anatomical organization (Williams and Goldman-Rakic, 1998) and may not be well represented by whole anatomically defined ROIs. For the cingulate cortex, the template used in the ROI approach was restricted to the ACC (based on Abi-Dargham *et al* (2002)),

while the voxel-wise template included the whole cingulate cortex. The significant cluster identified in the voxel-wise analyses lied in the ACC, as well as other regions of the cingulate, and as a result the post-smoking reduction in BP_{ND} was more robust in the voxel-wise analysis, which included the whole cingulate (see Figure 2b and Supplementary Figure 1), thus demonstrating the value of such an approach. A limitation of this approach, however, is that when compared with whole ROI-extracted values, cluster extracted values tended to be lower (see Figure 2b and Supplementary Figure 1). Despite low-binding values, average TACs extracted from significant clusters reliably fitted with SRTM (covariance of the fit $<10\%$) and, importantly, the results were supported by the follow-up investigation in anatomically defined ROIs (see Supplementary Figure 1).

The sample size of the current study ($n=10$) was sufficient to detect smoking effects on [^{11}C]-FLB-457 BP_{ND}. Future studies should use a larger sample size to better explore the relationship between cortical DA and the behavioral effects of tobacco smoking, particularly on cognitive function. A larger sample would also allow investigation of potential factors influencing inter-individual variability such as gender and gene variants including COMT Val^{158}Met (Loughead *et al*, 2009; Wing *et al*, 2013a). We chose to study a non-psychiatric population of smokers in this initial study but an important next step will be to implement this methodology in smokers selected for their vulnerability to nicotine's cognitive effects, such as patients with schizophrenia. In addition, this study was designed to examine the effects of the act of tobacco smoking rather than nicotine per se on cortical DA release. This approach was chosen to attempt to elicit the maximum DA release by encompassing pharmacological (eg, nicotine) and non-pharmacological factors (eg, conditioned cues associated with smoking). Furthermore, we believe it is of important clinical relevance to study cortical DA under abstinence and smoking conditions, and thus its potential role in maintaining smoking behavior. This was therefore an appropriate starting point for a proof-of concept study. However, in future it will be important to dissociate the effects of tobacco cues *vs* the pharmacological effects of tobacco and also the effects of individual components of tobacco smoke, eg, by studying the effects of denicotinized cigarettes and nicotine replacement therapies. It will also be of interest to determine the effects of nicotine on cortical DA in non-smoking nicotine-naive subjects, which may provide insights its role in the initiation of smoking.

In conclusion, this study demonstrates for the first time that increases in DA levels produced by tobacco smoking can be detected in cortical brain regions in humans using [^{11}C]-FLB-457 PET imaging. Changes in [^{11}C]-FLB-457 BP_{ND} were most robust in a larger medial cluster, which included the cingulate gyrus, with some evidence for effects in the left ACC/Med. FG, bilateral PFC, bilateral amygdala, and the left insula. Activation of these brain regions have been associated with tobacco craving, cognition, and relapse in fMRI studies, and thus warrant further investigation in larger and more diverse samples. [^{11}C]-FLB-457 PET imaging may prove to be a useful tool to investigate individual differences in tobacco addiction severity and relapse vulnerability in relation to cortical DA function.

FUNDING AND DISCLOSURE

Dr George reports that in the past 12 months he has been a consultant to Pfizer on smoking cessation medications, and recipient of grant support for multi-center and investigator-initiated studies from Pfizer, as well as a member of a Data Monitoring Committee (DMC) for Novartis. This research was supported by the Canada Foundation for Innovation Research Hospital Fund (CFI-RHF 16014, to T.P.G.) and the Canada Foundation for Innovation Leader Opportunity Fund (CFI-LOF 19229, to T.P.G.), CIHR Operating Grant MOP115145 (to T.P.G.), and the Chair in Addiction Psychiatry from the University of Toronto (to T.P.G.). The funding agencies had no role in the design of the study or the analysis and interpretation of the findings. Drs Wing, Payer, Houle and Boileau have nothing to disclose.

ACKNOWLEDGEMENTS

We thank the staff of the CAMH Research Imaging Centre for their support with the imaging procedures; Marleen Pronker, Stela Penalva, and Ilona Gorbovskaya for assistance in maintaining the study database; Dr Ariel Graff for psychiatric and medical support during the study; and Dr Cristiana Stefan (Director, Clinical Laboratories and Diagnostic Services, Centre for Addiction and Mental Health, Toronto) for assistance with nicotine and cotinine analyses.

REFERENCES

Aalto S, Bruck A, Laine M, Nagren K, Rinne JO (2005). Frontal and temporal dopamine release during working memory and attention tasks in healthy humans: a positron emission tomography study using the high-affinity dopamine D2 receptor ligand [11C]FLB 457. *J Neurosci* **25**: 2471–2477.

Abi-Dargham A, Mawlawi O, Lombardo I, Gil R, Martinez D, Huang Y *et al* (2002). Prefrontal dopamine D1 receptors and working memory in schizophrenia. *J Neurosci* **22**: 3708–3719.

Ashare RL, Falcone M, Lerman C (2014). Cognitive function during nicotine withdrawal: Implications for nicotine dependence treatment. *Neuropharmacology* **76**(Pt B): 581–591.

Asselin MC, Montgomery AJ, Grasby PM, Hume SP (2007). Quantification of PET studies with the very high-affinity dopamine D2/D3 receptor ligand [11C]FLB 457: re-evaluation of the validity of using a cerebellar reference region. *J Cereb Blood Flow Metab* **27**: 378–392.

Azizian A, Nestor LJ, Payer D, Monterosso JR, Brody AL, London ED (2010). Smoking reduces conflict-related anterior cingulate activity in abstinent cigarette smokers performing a Stroop task. *Neuropsychopharmacology* **35**: 775–782.

Barrett SP, Boileau I, Okker J, Pihl RO, Dagher A (2004). The hedonic response to cigarette smoking is proportional to dopamine release in the human striatum as measured by positron emission tomography and [11C]raclopride. *Synapse* **54**: 65–71.

Beck AT, Steer RA, Ball R, Ranieri W (1996). Comparison of Beck Depression Inventories -IA and -II in psychiatric outpatients. *J Pers Assess* **67**: 588–597.

Bernert JT Jr., Turner WE, Pirkle JL, Sosnoff CS, Akins JR, Waldrep MK *et al* (1997). Development and validation of sensitive method for determination of serum cotinine in smokers and nonsmokers by liquid chromatography/atmospheric pressure ionization tandem mass spectrometry. *Clin Chem* **43**: 2281–2291.

Boileau I, Payer D, Chugani B, Lobo DS, Houle S, Wilson AA *et al* (2014). *In vivo* evidence for greater amphetamine-induced dopamine release in pathological gambling: a positron emission tomography study with [(11)C]-(+)-PHNO. *Mol Psychiatry* **19**: 1305–1313.

Brody AL, Mandelkern MA, London ED, Childress AR, Lee GS, Bota RG *et al* (2002). Brain metabolic changes during cigarette craving. *Arc Gen Psychiatry* **59**: 1162–1172.

Brody AL, Mandelkern MA, Olmstead RE, Allen-Martinez Z, Scheibal D, Abrams AL *et al* (2009). Ventral striatal dopamine release in response to smoking a regular vs a denicotinized cigarette. *Neuropsychopharmacology* **34**: 282–289.

Brody AL, Olmstead RE, London ED, Farahi J, Meyer JH, Grossman P *et al* (2004). Smoking-induced ventral striatum dopamine release. *Am J Psychiatry* **161**: 1211–1218.

Castner SA, Goldman-Rakic PS (2004). Enhancement of working memory in aged monkeys by a sensitizing regimen of dopamine D1 receptor stimulation. *J Neurosci* **24**: 1446–1450.

Delforge J, Bottlaender M, Loc'h C, Guenther I, Fuseau C, Bendriem B *et al* (1999). Quantitation of extrastriatal D2 receptors using a very high-affinity ligand (FLB 457) and the multi-injection approach. *J Cereb Blood Flow Metab* **19**: 533–546.

Di Chiara G (2000). Role of dopamine in the behavioural actions of nicotine related to addiction. *Eur J Pharmacology* **393**: 295–314.

Domino EF, Tsukada H (2009). Nicotine sensitization of monkey striatal dopamine release. *Eur J Pharmacology* **607**: 91–95.

First MB, Spitzer RL, Gibbon M, Williams JBW (1996). Structured Clinical Interview for DSM-IV Axis I Disorders, Clinician Version (SCID-CV) Washington, D.C.: American Psychiatric Press, Inc.

Gallezot JD, Kloczynski T, Weinzimmer D, Labaree D, Zheng MQ, Lim K *et al* (2014). Imaging nicotine- and amphetamine-induced dopamine release in rhesus monkeys with [(11)C]PHNO vs [(11)C]raclopride PET. *Neuropsychopharmacology* **39**: 866–874.

Garris PA, Wightman RM (1994). Different kinetics govern dopaminergic transmission in the amygdala, prefrontal cortex, and striatum: an in vivo voltammetric study. *J Neuroscience* **14**: 442–450.

George TP, Verrico CD, Picciotto MR, Roth RH (2000). Nicotinic modulation of mesoprefrontal dopamine neurons: pharmacologic and neuroanatomic characterization. *J Pharmacol Exper Ther* **295**: 58–66.

Gunn RN, Lammertsma AA, Hume SP, Cunningham VJ (1997). Parametric imaging of ligand-receptor binding in PET using a simplified reference region model. *NeuroImage* **6**: 279–287.

Halldin C, Farde L, Hogberg T, Mohell N, Hall H, Suhara T *et al* (1995). Carbon-11-FLB 457: a radioligand for extrastriatal D2 dopamine receptors. *J Nuclear Med* **36**: 1275–1281.

Heatherton TF, Kozlowski LT, Frecker RC, Fagerström KO (1991). The Fagerström Test for Nicotine Dependence: a revision of the Fagerström Tolerance Questionnaire. *Br J Addict* **86**: 1119–1127.

Heishman SJ, Kleykamp BA, Singleton EG (2010). Meta-analysis of the acute effects of nicotine and smoking on human performance. *Psychopharmacology (Berl)* **210**: 453–469.

Hughes JR, Hatsukami D (1986). Signs and symptoms of tobacco withdrawal. *Arch Gen Psychiatry* **43**: 289–294.

Ito H, Sudo Y, Suhara T, Okubo Y, Halldin C, Farde L (2001). Error analysis for quantification of [(11)C]FLB 457 binding to extrastriatal D(2) dopamine receptors in the human brain. *NeuroImage* **13**: 531–539.

Janes AC, Pizzagalli DA, Richardt S, de BFB, Chuzi S, Pachas G *et al* (2010a). Brain reactivity to smoking cues prior to smoking cessation predicts ability to maintain tobacco abstinence. *Biol Psychiatry* **67**: 722–729.

Janes AC, Pizzagalli DA, Richardt S, Frederick Bde B, Holmes AJ, Sousa J *et al* (2010b). Neural substrates of attentional bias for smoking-related cues: an FMRI study. *Neuropsychopharmacology* **35**: 2339–2345.

Janes AC, Ross RS, Farmer S, Frederick BB, Nickerson LD, Lukas SE *et al* (2013). Memory retrieval of smoking-related images induce greater insula activation as revealed by an fMRI-based delayed matching to sample task. *Addict Biol* doi:10.1111/adb.12112; e-pub ahead of print.

Kim SE, Han SM (2009). Nicotine- and methamphetamine-induced dopamine release evaluated with in-vivo binding of radiolabelled raclopride to dopamine D2 receptors: comparison with in-vivo microdialysis data. *Int J Neuropsychopharmacol* **12**: 833–841.

Ko JH, Ptito A, Monchi O, Cho SS, Van Eimeren T, Pellecchia G *et al* (2009). Increased dopamine release in the right anterior cingulate cortex during the performance of a sorting task: a [11C]FLB 457 PET study. *NeuroImage* **46**: 516–521.

Lammertsma AA, Hume SP (1996). Simplified reference tissue model for PET receptor studies. *NeuroImage* **4**(3 Pt 1): 153–158.

Laruelle M (2000). Imaging synaptic neurotransmission with in vivo binding competition techniques: a critical review. *J Cereb Blood Flow Metab* **20**: 423–451.

Le Foll B, Guranda M, Wilson AA, Houle S, Rusjan PM, Wing VC *et al* (2014). Elevation of dopamine induced by cigarette smoking: novel insights from a [(11)C]-(+)-PHNO PET study in humans. *Neuropsychopharmacology* **39**: 415–424.

Levin ED, McClernon FJ, Rezvani AH (2006). Nicotinic effects on cognitive function: behavioral characterization, pharmacological specification, and anatomic localization. *Psychopharmacology (Berl)* **184**: 523–539.

Lieberman MD, Cunningham WA (2009). Type I and type II error concerns in fMRI research: re-balancing the scale. *Soc Cogn Affect Neurosci* **4**: 423–428.

Livingstone PD, Srinivasan J, Kew JNC, Dawson LA, Gotti C, Moretti M *et al* (2009). alpha7 and non-alpha7 nicotinic acetylcholine receptors modulate dopamine release in vitro and in vivo in the rat prefrontal cortex. *Eur J Neurosci* **29**: 539–550.

Loughead J, Wileyto EP, Valdez JN, Sanborn P, Tang K, Strasser AA *et al* (2009). Effect of abstinence challenge on brain function and cognition in smokers differs by COMT genotype. *Mol Psychiatry* **14**: 820–826.

Maldjian JA, Laurienti PJ, Kraft RA, Burdette JH (2003). An automated method for neuroanatomic and cytoarchitectonic atlas-based interrogation of fMRI data sets. *NeuroImage* **19**: 1233–1239.

Mansvelder HD, De Rover M, McGehee DS, Brussaard AB (2003). Cholinergic modulation of dopaminergic reward areas: upstream and downstream targets of nicotine addiction. *Eur J Pharmacol* **480**: 117–123.

Marenco S, Carson RE, Berman KF, Herscovitch P, Weinberger DR (2004). Nicotine-induced dopamine release in primates measured with [11C]raclopride PET. *Neuropsychopharmacology* **29**: 259–268.

Marshall DL, Redfern PH, Wonnacott S (1997). Presynaptic nicotinic modulation of dopamine release in the three ascending pathways studied by in vivo microdialysis: comparison of naive and chronic nicotine-treated rats. *J Neurochem* **68**: 1511–1519.

Mukherjee J, Yang ZY, Das MK, Brown T (1995). Fluorinated benzamide neuroleptics–III. Development of (S)-N-[(1-allyl-2-pyrrolidinyl)methyl]-5-(3-[18F]fluoropropyl)-2, 3-dimethoxybenzamide as an improved dopamine D-2 receptor tracer. *Nuclear Med Biol* **22**: 283–296.

Nagano-Saito A, Dagher A, Booij L, Gravel P, Welfeld K, Casey KF *et al* (2013). Stress-induced dopamine release in human medial prefrontal cortex–18F-fallypride/PET study in healthy volunteers. *Synapse* **67**: 821–830.

Narendran R, Frankle WG, Mason NS, Rabiner EA, Gunn RN, Searle GE *et al* (2009). Positron emission tomography imaging of amphetamine-induced dopamine release in the human cortex: a comparative evaluation of the high affinity dopamine D2/3

radiotracers [11C]FLB 457 and [11C]fallypride. *Synapse* **63**: 447–461.

Narendran R, Himes M, Mason NS (2013). Reproducibility of post-amphetamine [11C]FLB 457 binding to cortical D2/3 receptors. *PloS One* **8**: e76905.

Narendran R, Jedema HP, Lopresti BJ, Mason NS, Gurnsey K, Ruszkiewicz J *et al* (2014). Imaging dopamine transmission in the frontal cortex: a simultaneous microdialysis and [(11)C]FLB 457 PET study. *Mol Psychiatry* **19**: 399.

Narendran R, Mason NS, Chen CM, Himes M, Keating P, May MA *et al* (2011a). Evaluation of dopamine D(2)/(3) specific binding in the cerebellum for the positron emission tomography radiotracer [(1)(1)C]FLB 457: implications for measuring cortical dopamine release. *Synapse* **65**: 991–997.

Narendran R, Mason NS, May MA, Chen CM, Kendro S, Ridler K *et al* (2011b). Positron emission tomography imaging of dopamine D(2)/(3) receptors in the human cortex with [(1)(1)C]FLB 457: reproducibility studies. *Synapse* **65**: 35–40.

Olsson H, Halldin C, Farde L (2004). Differentiation of extrastriatal dopamine D2 receptor density and affinity in the human brain using PET. *NeuroImage* **22**: 794–803.

Paulson PE, Robinson TE (1994). Relationship between circadian changes in spontaneous motor activity and dorsal versus ventral striatal dopamine neurotransmission assessed with on-line microdialysis. *Behav Neurosci* **108**: 624–635.

Rusjan P, Mamo D, Ginovart N, Hussey D, Vitcu I, Yasuno F *et al* (2006). An automated method for the extraction of regional data from PET images. *Psychiatry Res* **147**: 79–89.

Sacco KA, Termine A, Seyal A, Dudas MM, Vessicchio JC, Krishnan-Sarin S *et al* (2005). Effects of cigarette smoking on spatial working memory and attentional deficits in schizophrenia: involvement of nicotinic receptor mechanisms. *Arch Gen Psychiatry* **62**: 649–659.

Schilstrom B, Nomikos GG, Nisell M, Hertel P, Svensson TH (1998). N-methyl-D-aspartate receptor antagonism in the ventral tegmental area diminishes the systemic nicotine-induced dopamine release in the nucleus accumbens. *Neuroscience* **82**: 781–789.

Sesack SR, Grace AA (2009). Cortico-basal ganglia reward network: microcircuitry. *Neuropsychopharmacology* **35**: 27–47.

Shotbolt P, Tziortzi AC, Searle GE, Colasanti A, van der Aart J, Abanades S *et al* (2012). Within-subject comparison of [(11)C]-(+)-PHNO and [(11)C]raclopride sensitivity to acute amphetamine challenge in healthy humans. *J Cereb Blood Flow Metab* **32**: 127–136.

Sobell LC, Sobell MB, Leo GI, Cancilla A (1988). Reliability of a timeline method: assessing normal drinkers' reports of recent drinking and a comparative evaluation across several populations. *Br J Addict* **83**: 394–402.

Sudo Y, Suhara T, Inoue M, Ito H, Suzuki K, Saijo T *et al* (2001). Reproducibility of [11 C]FLB 457 binding in extrastriatal regions. *Nuclear Med Commun* **22**: 1215–1221.

Tiffany ST, Drobes DJ (1991). The development and initial validation of a questionnaire on smoking urges. *Br J Addict* **86**: 1467–1476.

Vilkman H, Kajander J, Nagren K, Oikonen V, Syvalahti E, Hietala J (2000). Measurement of extrastriatal D2-like receptor binding with [11C]FLB 457–a test-retest analysis. *Eur J Nuclear Med* **27**: 1666–1673.

Williams SM, Goldman-Rakic PS (1998). Widespread origin of the primate mesofrontal dopamine system. *Cereb Cortex* **8**: 321–345.

Wing VC, Tang YL, Sacco KA, Cubells JF, George TP (2013a). Effect of COMT Val(158)Met genotype on nicotine withdrawal-related cognitive dysfunction in smokers with and without schizophrenia. *Schizophr Res* **150**: 602–603.

Wing VC, Wass CE, Bacher I, Rabin RA, George TP (2013b). Varenicline modulates spatial working memory deficits in smokers with schizophrenia. *Schizophr Res* **149**: 190–191.

Wing VC, Wass CE, Soh DW, George TP (2012). A review of neurobiological vulnerability factors and treatment implications for comorbid tobacco dependence in schizophrenia. *Ann N Y Acad Sci* **248**: 89–106.

Wood DM, Mould MG, Ong SB, Baker EH (2005). "Pack year" smoking histories: what about patients who use loose tobacco? *Tob Control* **14**: 141–142.

Zachary RA, Paulson MJ, Gorsuch Y (1985). Estimating WAIS IQ from the Shipley Institute of Living Scale using continuously adjusted age norms. *J Clin Psychol* **41**: 820–831.

Zubieta JK, Heitzeg MM, Xu Y, Koeppe RA, Ni L, Guthrie S *et al* (2005). Regional cerebral blood flow responses to smoking in tobacco smokers after overnight abstinence. *Am J Psychiatry* **162**: 567–577.

Supplementary Information accompanies the paper on the Neuropsychopharmacology website (http://www.nature.com/npp)